

Continuous measurement of a charge qubit: inelastic tunnelling and the absence of current oscillations

T.M. Stace¹ and S. D. Barrett^{1,2}

¹*Cavendish Laboratory, University of Cambridge, Madingley Road, Cambridge CB3 0HE, UK**

²*Hewlett Packard Laboratories, Filton Road, Stoke Gifford Bristol, BS34 8QZ†*

(Dated: February 20, 2004)

We study the dynamics of a charge qubit, consisting of a single electron in a double well potential, coupled to a point-contact (PC) electrometer using the quantum trajectories formalism. In contrast with previous predictions, we show that in the sub-Zeno regime, coherent oscillations in the detector output are suppressed by inelastic processes in the PC. They also reduce the detector efficiency. We show that the sub-Zeno dynamics are divided into two regimes: low- and high-bias in which the PC current power spectra show markedly different behaviour. To further illustrate the division between the regimes and the inefficiency of the detector, we present simulated quantum trajectories of the conditional qubit and detector dynamics. We describe how quantum non-demolition measurements in an arbitrary basis may be achieved in the sub-Zeno regime.

PACS numbers: 73.63.Kv 85.35.Be, 03.65.Ta, 03.67.Lx

I. INTRODUCTION

Single shot quantum measurement of mesoscopic systems is recognised as an important goal. Fundamentally, it will allow us to make time-resolved observations of quantum mechanical effects in such systems, and practically it will be a necessary component in the construction of solid-state quantum information processors (QIP). There are numerous proposals for implementing QIP in solid state systems, using doped silicon¹, electrostatically defined quantum dots² and superconducting boxes³. In these proposals, the output of the QIP is determined by measuring the position of a single electron or Cooper pair. Single electrons hopping onto single quantum dots have been observed on a microsecond time scale using single-electron transistors (SET)⁴. Ensemble measurements of a double well system (qubit) have been demonstrated in superconducting devices⁵. So far, single shot qubit measurements remain elusive.

It is therefore important to consider the measurement of single electron qubits by sensitive electrometers. Two possible electrometers have been discussed to date: SETs (see e.g. Makhlin et al.³) and point contacts (PCs)⁶⁻¹⁴. PCs have been shown to be sensitive charge detectors¹⁵⁻¹⁸, and are the focus of this work. Figure 1 illustrates the physical system we consider here, with a PC (represented by two Fermi seas separated by a tunnel barrier) in close proximity to one of the double well minima. Despite the apparent simplicity of this system it exhibits a rich range of behaviour.

There are several energy scales of relevance: the splitting of the qubit eigenstates, ϕ , the bias voltage applied across the PC, $eV = \mu_S - \mu_D$, and the measurement induced dephasing rate, Γ_d , due to the different currents through the PC that result for different localised qubit electron states. These three energies define three distinct measurement regimes

1. low-bias regime, where $\Gamma_d/2 \ll eV < \phi$.
2. high-bias regime, where $\Gamma_d/2 \ll \phi < eV$.
3. quantum Zeno limit, where $\phi \ll \Gamma_d/2 \ll eV$.

In the quantum Zeno limit, frequent weak measurements localise the qubit, suppressing its dynamics^{6,10}. To date, analyses have not discussed the low- bias regime. It has been predicted that in the limit, $\Gamma_d/2 \ll \phi$, which we refer to as the sub-Zeno limit, coherent oscillations due to the quantum dynamics of the qubit will be observed in the power spectrum of the current through the PC^{6,9,10,13}. This is closely related to the assumption that the PC is an efficient detector, that is, no information about the qubit is lost by the detector.

We present a detailed analysis of the sub-Zeno limit, showing the sharp difference in behaviour between the low- and high- bias regimes, and we show that previously predicted coherent oscillations are suppressed by inelastic tunnelling of electrons through the PC. These inelastic processes incoherently excite or relax the qubit, yet are not in general experimentally distinguishable using current measurement from elastic tunnelling processes and thus result in fluctuations that destroy the predicted coherent oscillations. The analysis also formally yields the boundary at which approximations leading to the Zeno effect are reasonable.

The paper begins with a derivation of an unconditional master equation for the joint system consisting of qubit and PC, highlighting the significance of the Fourier decomposition of the interaction Hamiltonian. We then present analytic

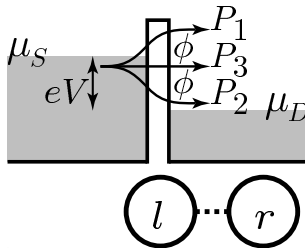


FIG. 1: Schematic of the qubit and PC showing lead energy bands. Electrons tunnelling from the source to the drain may do so elastically or inelastically, depicted by arrows. Different transitions induce different jumps, P_i , on the qubit.

solutions to this master equation, as well as an unravelling of the master equation applicable to the measurement records available in a PC current measurement. Following this, we derive the steady state power spectrum and demonstrate formally the close analogy between the PC bias voltage and a heat bath. We end the analysis with some sample trajectories showing possible measurement outcomes. We conclude the paper with a discussion of our results.

II. SYSTEM HAMILTONIAN

We model the double well system as a two level system, on the basis that the two lowest energy eigenstates, $|e\rangle$ and $|g\rangle$ of the double well system are well separated from higher lying single particle energy eigenstates. We write these eigenstates as

$$\begin{aligned} |e\rangle &= -\sin(\theta/2)|l\rangle + \cos(\theta/2)|r\rangle, \\ |g\rangle &= \sin(\theta/2)|r\rangle + \cos(\theta/2)|l\rangle, \end{aligned}$$

where $|l\rangle$ and $|r\rangle$ are the left and right localised states respectively. The Hamiltonian for the double well system, its interaction with the PC leads and the lead Hamiltonian is

$$H_{\text{sys}} = -\frac{\Delta}{2}\sigma_x - \frac{\epsilon}{2}\sigma_z = -\phi\sigma_z^{(e)}/2, \quad (1)$$

$$H_{\text{meas}} = \sum_{k,q} (T_{k,q} + \chi_{k,q}\sigma_z) a_{D,q}^\dagger a_{S,k} + \text{H.c.} \quad (2)$$

$$H_{\text{leads}} = H_S + H_D = \sum_k \omega_k (a_{S,k}^\dagger a_{S,k} + a_{D,k}^\dagger a_{D,k}) \quad (3)$$

where $\sigma_x = |l\rangle\langle r| + |r\rangle\langle l|$, $\sigma_z = |l\rangle\langle l| - |r\rangle\langle r|$, $\theta = \tan^{-1}(\frac{\Delta}{\epsilon})$, $\phi = \sqrt{\Delta^2 + \epsilon^2}$ and $\sigma_z^{(e)} = |g\rangle\langle g| - |e\rangle\langle e|$. We adopt the convention that $\chi_{k,q} < 0$ so that the left well is nearest the PC. When $\theta = 0$ the energy eigenstates coincide with the localised states, since tunnelling is effectively switched off. At $\theta = \pi/2$, the tunnelling rate, Δ , dominates the bias, ϵ , so the eigenstates are the completely delocalised states.

III. MASTER EQUATION

The von Neumann equation for the density matrix, R , of the bath and system is

$$\dot{R}(t) = -i[H_{\text{Tot}}, R]. \quad (4)$$

To derive the master equation for the reduced density operator, ρ , of the double well system we transform to an interaction picture with respect to the free Hamiltonian $H_0 = H_{\text{sys}} + H_{\text{leads}}$, $H_I(t) = e^{iH_0 t} H_{\text{Tot}} e^{-iH_0 t} - H_0 = e^{iH_0 t} H_{\text{meas}} e^{-iH_0 t}$, expand the von Neumann equation to second order and trace over the lead modes, i.e.

$$\dot{\rho}_I(t) = \text{Tr}_{S,D} \{ -i[H_I(t), R(t)] - [H_I(t), \int_0^t dt' [H_I(t'), R(t')]] \}, \quad (5)$$

where

$$H_1(t) = \sum_{k,q} e^{i(\omega_k - \omega_q)t} (T_{k,q} + \chi_{k,q} \sigma_z(t)) a_{D,q}^\dagger a_{S,k} + \text{H.c.} \equiv \sum_{k,q} S_{k,q}(t) a_{D,q}^\dagger a_{S,k} + \text{H.c.}, \quad (6)$$

$$\text{and } \sigma_z(t) = \frac{1}{2} \begin{pmatrix} \cos(\theta) & e^{-it\phi} \sin(\theta) \\ e^{it\phi} \sin(\theta) & -\cos(\theta) \end{pmatrix} \quad (7)$$

and $S_{k,q}(t)$ is a time dependent system operator that may be written as a discrete Fourier decomposition $S_{k,q}(t) = \sum_n e^{-i(\omega_k - \omega_q + \omega_n)t} P_n$ for some time independent operators P_n and frequencies ω_n . We can write the operator $S_{k,q}(t)$ explicitly as

$$S_{k,q}(t) = e^{-it(\omega_k - \omega_q)} (e^{-it\phi} P_1 + e^{it\phi} P_2 + P_3), \quad (8)$$

where $P_1 = P_2^\dagger = \frac{\chi_{00} \sin(\theta)}{2} |g\rangle\langle e|$, $P_3 = (T_{00} + \frac{\chi_{00} \cos(\theta)}{2} \sigma_z^{(e)})$ and we have assumed that $T_{k,q} = T_{00}$ and $\chi_{k,q} = \chi_{00}$ are constant.

The form of $S_{k,q}(t)$ indicates that there are three possible jump processes, indicated in Fig. 1. P_3 is associated with elastic tunnelling of electrons through the PC. P_1 and P_2 are associated respectively with inelastic excitation and relaxation of electrons tunnelling through the PC accompanied by an energy transfer ϕ . This energy is provided by the qubit which relaxes or excites in response. Inelastic transitions in similar systems have been described in¹⁹, which calculated the current power spectrum through an *open* double well system due to shot noise through a nearby PC.

Assuming the leads are always near thermal equilibrium, $\text{Tr}_{S,D}\{a_{i,k}^\dagger R(t)\} = \text{Tr}_{S,D}\{a_{i,k} R(t)\} = 0$ and $\text{Tr}_{S,D}\{a_{i,k}^\dagger a_{n,k} R(t)\} = \delta_{i,j} f_i(\omega_k) \rho(t)$, where $i, j \in \{L, R\}$ and f_i is the Fermi distribution for lead i . We also make the common assumption²⁰ that if the lead correlation time is much shorter than other time scales, then the lower limit on the time integral in Eq. (5) may be set to $-\infty$. Equation (5) becomes

$$\begin{aligned} \dot{\rho}_I(t) \approx & - \int_{-\infty}^t dt' \int d\omega_k \int d\omega_q g_S(\omega_k) g_D(\omega_q) f_S(\omega_k) (1 - f_D(\omega_q)) \\ & \times (S(t)^\dagger S(t') \rho_I(t') - S(t) \rho_I(t') S(t')^\dagger - S(t') \rho_I(t') S(t)^\dagger + \rho_I(t') S(t')^\dagger S(t)) \\ & - \int_{-\infty}^t dt' \int d\omega_k \int d\omega_q g_S(\omega_k) g_D(\omega_q) f_D(\omega_q) (1 - f_S(\omega_k)) \\ & \times (S(t) S(t')^\dagger \rho_I(t') - S(t)^\dagger \rho_I(t') S(t') - S(t')^\dagger \rho_I(t') S(t) + \rho_I(t') S(t') S(t)^\dagger), \end{aligned} \quad (9)$$

where we have made the standard replacement $\sum_k \rightarrow \int d\omega_k g_{S(D)}(\omega_k)$ where $g_{S(D)}(\omega_k)$ is the density of states for lead $S(D)$ which we will hereafter assume is a constant, $g_{S(D)}$, in the energy range of interest.

We wish to evaluate the integrals in Eq. (9) at zero temperature, so to show the method and approximations used, we evaluate a particular term in Eq. (9) using the Fourier decomposition of $S(t)$:

$$\begin{aligned} & \sum_{k,q} f_S(\omega_k) (1 - f_D(\omega_q)) \int_{-\infty}^t dt' S(t) \rho_I(t') S^\dagger(t') \\ & = \sum_{mn} \int d\omega_k \int d\omega_q g_S g_D f_S(\omega_k) (1 - f_D(\omega_q)) \int_{-\infty}^t dt' e^{-i(\omega_k - \omega_q + \omega_m)t} e^{i(\omega_k - \omega_q + \omega_n)t'} P_m \rho_I(t') P_n^\dagger, \\ & \approx \pi g_S g_D \sum_{mn} \int d\omega_k \int d\omega_q f_S(\omega_k) (1 - f_D(\omega_q)) \delta(\omega_k - \omega_q + \omega_n) e^{i(\omega_m - \omega_n)t} P_m \rho_I(t) P_n^\dagger, \\ & \approx \pi g_S g_D \sum_n \int d\omega_k f_S(\omega_k) (1 - f_D(\omega_k + \omega_n)) P_n \rho_I(t) P_n^\dagger. \\ & = \pi g_S g_D \sum_n \Theta(\mu_S - \mu_D + \omega_n) P_n \rho_I(t) P_n^\dagger, \end{aligned} \quad (10)$$

where $\Theta(x) = (x + |x|)/2$ is the ramp function and μ_i is the chemical potential of lead i . The first equality follows from substituting the Fourier decomposition of $S(t)$, the second equality follows from evaluating the integral over t' (see Appendix A), which is equivalent to making the replacement $\rho_I(t') \rightarrow \rho_I(t)$, the third (approximate) equality we have made a rotating-wave approximation (RWA), where we make the replacement $e^{i(\omega_n - \omega_m)t} \rightarrow \delta_{m,n}$, and finally we integrate over ω_k . The RWA is reasonable as long as $\phi \gg \nu^2 eV$, where $\nu = \sqrt{\pi g_S g_D / 2 \chi_{00}}$ is a small quantity. This

is justified when we come to integrate the master equation where terms with $n \neq m$ are rotating sufficiently rapidly to vanish. Using the same arguments on each term in Eq. (9) results in the general form of the master equation

$$\dot{\rho}_I(t) = 2\pi g_S g_D \sum_n \left(\mathcal{D}[\sqrt{\Theta(eV + \omega_n)} P_n] \rho_I(t) + \mathcal{D}[\sqrt{\Theta(-eV - \omega_n)} P_n^\dagger] \rho_I(t) \right), \quad (11)$$

where $V = \mu_S - \mu_D$ is the bias applied across the PC, $\mathcal{D}[B]\rho = \mathcal{J}[B]\rho - \mathcal{A}[B]\rho$, $\mathcal{J}[B]\rho = B\rho B^\dagger$ and $\mathcal{A}[B]\rho = \frac{1}{2}(B^\dagger B\rho + \rho B^\dagger B)$.

We note that the RWA breaks down in the opposite regime, $\phi \ll \nu^2 eV$, called the quantum Zeno regime. In this regime an alternate approximation is accurate, which also amounts to a RWA, where we set $e^{i\phi t} \rightarrow 1$. In this limit, $S(t) = e^{-i\Delta\omega t}(T_{00} + \chi_{00}\sigma_z(0))$ has only one Fourier component, and we regain the master equation of Goan and Milburn⁶. We note that in this limit we can make the replacement $\sigma_z(t) \rightarrow \sigma_z(0)$, as in⁶, but the correct limit for which this is true is not $\phi \ll eV$ (see ref 44 of⁶) but $\phi \ll \nu^2 eV$ as mentioned above, which is a much tighter limit.

We will unravel the master equation so that we can describe the evolution of the system conditioned on current measurements. To do this, we follow Goan et al.⁷ by writing the master equation in its most general form, using the identity

$$-\mathcal{D}[B]\rho(t) = [(\Gamma_n^* B^\dagger - \Gamma_n B)/2, \rho(t)] - \sum_n \mathcal{D}[B + \Gamma_n]\rho(t). \quad (12)$$

Thus, the most general unravelling of Eq. (11) requires us to make the replacement $P_n \rightarrow P'_n = P_n + \Gamma_n$ for some scalar Γ_n , and a redefinition

$$H_{\text{sys}} \rightarrow H'_{\text{sys}} = H_{\text{sys}} + \frac{i}{2} \sum_n (eV + \omega_n)(\Gamma_n^* P_n^\dagger - \Gamma_n P_n). \quad (13)$$

We may transform the master equation, Eq. (11), back to a Schrödinger picture to reinstate the free dynamics of the double well system. It conveniently turns out that the transformation of the P_n 's back to the Schrödinger picture merely multiplies them by the unitary factor $e^{i\omega_n t}$. The Lindblad superoperators are invariant under such a transformation, so in the Schrödinger picture

$$\dot{\rho}(t) = -i[H'_{\text{sys}}, \rho(t)] + \sum_n (\text{H}(eV + \omega_n)\mathcal{D}[c_n]\rho(t) + \text{H}(-eV - \omega_n)\mathcal{D}[c_n^\dagger]\rho(t)) \equiv \mathcal{L}\rho(t), \quad (14)$$

where $\text{H}(x)$ is the unit step function. For convenience, we have defined $c_n = \sqrt{\Theta(eV + \omega_n)} P'_n$, so that

$$c_1 = \nu\sqrt{eV + \phi}\sin(\theta)(|g\rangle\langle e| + \gamma_1), \quad (15)$$

$$c_2 = \nu\sqrt{|eV - \phi|}\sin(\theta)(|e\rangle\langle g| + \gamma_2), \quad (16)$$

$$c_3 = \nu\sqrt{eV}\cos(\theta)\sigma_z^{(e)} + \mathcal{T}\sqrt{eV}, \quad (17)$$

for some constants, $\gamma_{1,2}, \mathcal{T}$. We will show later, on physical grounds, that $\gamma_{1,2} = 0$ and $\mathcal{T} = \sqrt{\pi g_S g_D / 2T_{00}}$.

IV. HIGH BIAS REGIME

In the high bias limit, $\text{H}(-eV - \omega_n) = 0$ for all n , and we assume this throughout this section. We write the Schrödinger picture master equation in this limit as

$$\dot{\rho}(t) = -i[H'_{\text{sys}}, \rho(t)] + \sum_n \mathcal{D}[c_n]\rho(t), \quad (18)$$

In order to determine γ_n for each jump operator, we must appeal to physical considerations. Firstly, we will use energy conservation arguments to show that $\gamma_1 = \gamma_2 = 0$. Secondly we will use the same kind of argument as used by Goan et al.⁷ to relate \mathcal{T} and ν to average currents through the point contact.

A. Analytic solution of unconditional master equation

We can solve the unconditional master equation in this regime exactly, and we present the solution in the interaction picture, since it contains the relevant decay time scales. With respect to the ordered basis $|g\rangle, |e\rangle$ it is given by

$$\rho_I(t) = \begin{pmatrix} \frac{eV+\phi}{2eV} - e^{-\Gamma_d \sin^2(\theta)t} (\rho_{ee}(0) + \frac{\phi-eV}{2eV}) & e^{-\Gamma_d(1+\cos^2(\theta))t} \rho_{ge}(0) \\ e^{-\Gamma_d(1+\cos^2(\theta))t} \rho_{eg}(0) & \frac{eV-\phi}{2eV} + e^{-\Gamma_d \sin^2(\theta)t} (\rho_{ee}(0) + \frac{\phi-eV}{2eV}) \end{pmatrix}, \quad (19)$$

where we have defined $\Gamma_d = 2\nu^2 eV$, consistent with⁶.

B. Compute $\gamma_{1,2}$

Experimentally we only have access to the current through the PC, and are unable to detect which of the three distinct jump process happen, since this would require us to measure the change in energy of electrons as they tunnel through the PC. Assuming that the ammeter has infinite bandwidth, we may write the conditional state of the system after a single electron has tunnelled through the PC at time t as the mixture

$$\tilde{\rho}_{1c}(t+dt) = dt \sum_n \mathcal{J}[c_n] \rho_c(t), \quad (20)$$

where the $\tilde{\rho}$ is the unnormalised density matrix, and the subscript c indicates that the state is conditional on the previous measurement record.

If the qubit starts off in an energy eigenstate of the system, then we expect that during the jump, the energy of the total system consisting of qubit plus leads should be conserved *on average*, that is $\langle H_{\text{Tot}}(t+dt) \rangle - \langle H_{\text{Tot}}(t) \rangle = \text{Tr} \{ H_{\text{Tot}}(\rho_{1c}(t+dt) - \rho_c(t)) \} = 0$. Immediately before a jump occurs, the joint system is in the state $R(t) = \rho_c(t) \otimes \rho_S \otimes \rho_D$, and immediately after a jump occurs (before thermalisation of the leads) the joint system will be in the (unnormalised) state $\tilde{R}(t+dt) = H_I(0)R(t)H_I(0)$. For the high bias case we are considering in this section, this is given by

$$\tilde{R}(t+dt) = \sum_{n,n'} \sum_{\omega,\omega'} c_n \rho_c(t) c_{n'}^\dagger \otimes a_{S,\omega} \rho_S a_{S,\omega'}^\dagger \otimes a_{D,\omega+\omega_n}^\dagger \rho_D a_{D,\omega'+\omega_n}, \quad (21)$$

where we are summing over energy indices, $\omega = \omega_k$, for notational convenience. Note that Eq. (21) is consistent with Eq. (20), i.e. $\text{Tr} \{ \tilde{R}(t+dt) \} = \tilde{\rho}_{1c}(t+dt)$, and if the initial state of the joint system were pure, then $R(t+dt)$ would correspond to a purification²¹ of $\rho_{1c}(t+dt)$. This is justified by considering the fact that, *in principle*, one could perform sensitive bolometric measurements on each of the leads before and after the jump, in order to determine which type of jump occurred. Therefore the state of the double well system after the jump is correlated with the state of the leads, so at least the diagonal elements in $\tilde{R}(t+dt)$ must agree with Eq. (21). We will only be interested in the diagonal elements, so Eq. (21) will suffice for our purposes.

The change in energy of the joint system during the jump is given by $\langle \Delta H_{\text{Tot}} \rangle = \text{Tr} \{ H_{\text{Tot}}(R(t+dt) - R(t)) \}$, and it may be shown that $\text{Tr} \{ H_{\text{meas}} R(t) \} = \text{Tr} \{ H_{\text{meas}} R(t+dt) \} = 0$ so that

$$\langle \Delta H_{\text{Tot}} \rangle = \text{Tr} \{ (H_{\text{sys}} + H_{\text{leads}})(R(t+dt) - R(t)) \}. \quad (22)$$

It is straightforward to show that $\text{Tr} \{ H_{\text{leads}} R(t) \} = \sum_{\omega=0}^{\mu_S} \omega + \sum_{\omega=0}^{\mu_D} \omega$, and we can show (see Appendix B)

$$\text{Tr} \{ H_S R(t+dt) \} = \frac{\text{Tr} \{ H_S \tilde{R}(t+dt) \}}{\text{Tr} \{ \tilde{R}(t+dt) \}} = \frac{\sum_n \text{Tr} \{ \mathcal{J}[c_n] \rho(t) \} \sum_{\omega'=\mu_D-\omega_n}^{\mu_S} \{ \sum_{\omega=0}^{\mu_S} \omega - \omega' \}}{\sum_n \sum_{\omega=\mu_D-\omega_n}^{\mu_S} \text{Tr} \{ \mathcal{J}[c_n] \rho(t) \}}, \quad (23)$$

and

$$\text{Tr} \{ H_D R(t+dt) \} = \frac{\text{Tr} \{ H_D \tilde{R}(t+dt) \}}{\text{Tr} \{ \tilde{R}(t+dt) \}} = \frac{\sum_n \text{Tr} \{ \mathcal{J}[c_n] \rho(t) \} \{ \sum_{\omega'=\mu_D-\omega_n}^{\mu_S} \sum_{\omega=0}^{\mu_D} \omega + \sum_{\omega'=\mu_D}^{\mu_S+\omega_n} 1 \}}{\sum_n \sum_{\omega=\mu_D-\omega_n}^{\mu_S} \text{Tr} \{ \mathcal{J}[c_n] \rho(t) \}}. \quad (24)$$

The summation over n reflects the fact that even though the state of the leads is correlated with the specific type of jump that occurs, the kinds of experimental measurements available to us do not distinguish between them, and so

we need to average over the possible final states given that a jump (of some kind) occurred. To evaluate the energy summations, we turn them into integrals according to the prescription $\sum_{\omega=a}^b \rightarrow g \int_a^b d\omega$, where g is the density of states, which we assume is a constant $g_S = g_D = g$ for both leads. We find

$$\langle \Delta H_{\text{leads}} \rangle = \text{Tr} \{ H_{\text{leads}}(R(t+dt) - R(t)) \} = \frac{\sum_n \text{Tr} \{ \mathcal{J}[c_n] \rho(t) \} \omega_n (\mu_S - \mu_D + \omega_n)}{\sum_n \text{Tr} \{ \mathcal{J}[c_n] \rho(t) \} (\mu_S - \mu_D + \omega_n)}. \quad (25)$$

In a similar manner, we calculate the expectation of the change in energy of the qubit system

$$\langle \Delta H_{\text{sys}} \rangle = \text{Tr} \{ H_{\text{sys}}(R(t+dt) - R(t)) \} = \frac{\sum_n \phi \langle e | \mathcal{J}[c_n] \rho(t) | e \rangle (\mu_S - \mu_D + \omega_n)}{\sum_n \text{Tr} \{ \mathcal{J}[c_n] \rho(t) \} (\mu_S - \mu_D + \omega_n)} - \phi \langle e | \rho(t) | e \rangle. \quad (26)$$

If the qubit system is in the state $|e\rangle$ or $|g\rangle$, then we expect the change in energy of the joint system to be zero. Setting $\rho(t) = |g\rangle\langle g|$ or $\rho(t) = |e\rangle\langle e|$, we find that

$$\langle \Delta H_{\text{Tot}} \rangle = \langle \Delta H_{\text{sys}} \rangle + \langle \Delta H_{\text{leads}} \rangle \propto \phi \sin^2(\theta) (|\gamma_1|^2 (eV + \phi)^2 - |\gamma_2|^2 (eV - \phi)^2). \quad (27)$$

Since eV and ϕ may be varied independently, $\langle \Delta H_{\text{Tot}} \rangle$ is zero only when $\gamma_1 = \gamma_2 = 0$. Furthermore, since c_3 is Hermitian, $\gamma_{1,2} = 0$ and Eq. (13) implies that $H'_{\text{sys}} = H_{\text{sys}}$.

C. Compute \mathcal{T}

We now need to relate \mathcal{T} to classical currents through the PC. There is a background current through the PC determined by T_{00} , whilst variations in the mean current, which form the detected signal are related to the coefficients of the jump operators, c_n . If we turn off the qubit tunnelling, so $\theta = 0$, then the qubit can be localised in the left or right well. In either case, a current flows through the PC, though it will be larger for the latter. We calculate \mathcal{T} from the average of these two currents. The current is related to the unnormalised, conditional density matrix according to

$$e \text{Tr} \{ \tilde{\rho}_{1c}(t+dt) \} = e \sum_n \text{Tr} \{ \mathcal{J}[c_n] \rho_c(t) \} dt = I(t) dt, \quad (28)$$

where $I(t)$ is the (conditional) instantaneous current through the PC depending on the state of the qubit, and e is the electron charge. If the qubit is in the energy eigenstate $|l\rangle$ ($|r\rangle$) then we expect a current $I_l = eT_l^2$ ($I_r = eT_r^2$) to flow through the PC. The mean and variation in the currents are $\bar{I}_{\text{loc}} = \frac{I_r + I_l}{2} = e \frac{T_r^2 + T_l^2}{2} = e(\mathcal{T}^2 + \nu^2)eV$ and $\delta I_{\text{loc}} = I_r - I_l = e(T_r^2 - T_l^2) = -4e\nu\mathcal{T}eV$. We therefore have the following conditions on \mathcal{T} and ν

$$\sum_n \text{Tr} \{ c_n |l\rangle \langle l| c_n^\dagger \} = eV(\mathcal{T} + \nu)^2 = T_l^2, \quad (29)$$

$$\sum_n \text{Tr} \{ c_n |r\rangle \langle r| c_n^\dagger \} = eV(\mathcal{T} - \nu)^2 = T_r^2. \quad (30)$$

Solving these two equations yields

$$\mathcal{T} = \frac{T_r + T_l}{2\sqrt{eV}} \quad \text{and} \quad \nu = \frac{T_l - T_r}{2\sqrt{eV}}. \quad (31)$$

For general values of θ we use Eq. (28) to write an expression for the instantaneous current that would result if an electron that were localised in the left or right well, i.e. if $\rho_c(t) = |l\rangle\langle l|$ or $|r\rangle\langle r|$ at some instant in time. The difference between these two currents indicates the capacity for the PC to discriminate between the localised states. We find that the average of the two currents is the same as above, $\bar{I}(\theta) = \bar{I}_{\text{loc}}$ but the difference between the currents is

$$\delta I(\theta) = \delta I_{\text{loc}} \cos^2(\theta) + O(\nu^2). \quad (32)$$

Notably, the variation in current between localised states vanishes when $\theta = \pi/2$, which indicates strongly that when the qubit is unbiased, so that the energy eigenstates are also parity eigenstates (i.e. $(|r\rangle \pm |l\rangle)/\sqrt{2}$), then the current through the PC does not make a measurement in the localised basis.

The fact that the current through the PC does not localise the electron is evident in the form of the jump operators, since when $\theta = \pi/2$, c_3 does not change the state of the qubit and the other two jump processes can only act to relax or excite the qubit.

D. Unravelling the master equation

When a jump occurs the qubit evolves discontinuously according to Eq. (20). Between jumps the state of the system evolves smoothly, and we derive the smooth dynamics by requiring consistency between the evolution averaged over zero and one jump in the interval $(t, t + dt)$ and Eq. (18). Averaging over conditional states after zero or one jump results in the unconditional master equation, so

$$\tilde{\rho}_{0c}(t + dt) + \tilde{\rho}_{1c}(t + dt) = [1 + dt\mathcal{L}]\rho_c(t). \quad (33)$$

Substituting Eq. (20) for $\tilde{\rho}_{1c}(t + dt)$ gives.

$$\tilde{\rho}_{0c}(t + dt) = \rho_c(t) - dt i[H_{\text{sys}}, \rho_c(t)] - dt \sum_n \mathcal{A}[c_n]\rho_c(t), \quad (34)$$

where $\mathcal{A}[B]\rho = \frac{1}{2}(B^\dagger B\rho + \rho B^\dagger B)$. We therefore conclude that the unnormalised qubit density matrix is governed by the smooth evolution

$$\dot{\tilde{\rho}}_{0c}(t) = -i[H_{\text{sys}}, \tilde{\rho}_{0c}(t)] - \sum_n \mathcal{A}[c_n]\tilde{\rho}_{0c}(t). \quad (35)$$

Since there is more than one jump term in this expression, we cannot unravel it further into a physically meaningful quantum trajectory for pure states.

V. LOW BIAS REGIME

In contrast to previous analyses of the system which assume that the qubit splitting is small compared with the PC bias, our analysis is valid in the low bias limit, $\phi > eV$, as well. The unconditional master equation in this regime is given by

$$\dot{\rho}(t) = -i[H'_{\text{sys}}, \rho(t)] + (\mathcal{D}[c_1]\rho(t) + \mathcal{D}[c_2^\dagger]\rho(t) + \mathcal{D}[c_3]\rho(t)). \quad (36)$$

In contrast to the high bias unravelling, when we come to unravel this low bias master equation, we will assume that a jump generated by c_2^\dagger is distinguishable from jumps generated by c_1 and c_3 (though these two are still mutually indistinguishable) using a current measurement. The reason is that when the qubit is subject to a jump of type c_2^\dagger , a lead electron hops from the drain to the source, opposite to jumps of type c_1 or c_3 from source to drain. Thus c_2^\dagger results in a current with opposite sign to the other two jump processes and so results in a current spike of opposite sign.

Following the same kind of reasoning as in Section IV B we find that $\gamma_1 = \gamma_2 = 0$. Thus c_1 and c_2^\dagger are related by a constant factor (see Eqs. (15) and (16)), $\mathcal{D}[c_1]\rho(t) + \mathcal{D}[c_2^\dagger]\rho(t) = 2\nu^2\phi^2 \sin^2(\theta)\mathcal{D}[|g\rangle\langle e|]\rho(t)$, so that the unconditional master equation has only two Lindblad terms.

The results of section IV C also carry over to the low-bias regime, and \mathcal{T} and ν are given by Eqs. (31).

A. Analytic solution of unconditional master equation

Again, we can solve the unconditional master equation in this regime exactly, and we present the solution in the interaction picture, since it contains the relevant decay time scales. With respect to the ordered basis $|g\rangle, |e\rangle$ it is given by

$$\rho_{\text{I}}(t) = \begin{pmatrix} 1 - e^{-2\nu^2\phi \sin^2(\theta)t} \rho_{ee}(0) & e^{-(2\Gamma_d \cos^2(\theta) + \nu^2\phi \sin^2(\theta))t} \rho_{ge}(0) \\ e^{-(2\Gamma_d \cos^2(\theta) + \nu^2\phi \sin^2(\theta))t} \rho_{ge}(0) & e^{-2\nu^2\phi \sin^2(\theta)t} \rho_{ee}(0) \end{pmatrix}. \quad (37)$$

Note that at $\phi = eV$, Eqs. (19) and (37) agree.

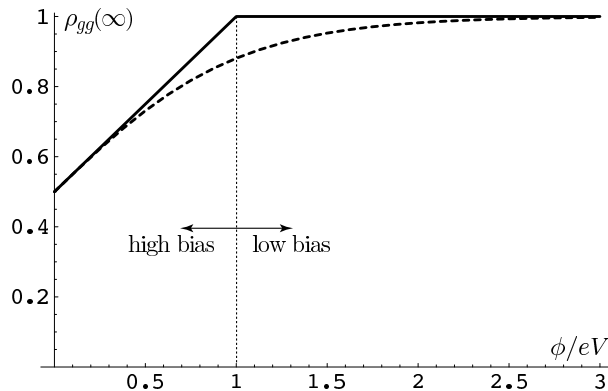


FIG. 2: Equilibrium ground state occupation probability for a qubit near a PC (solid), and the thermal equilibrium ground state occupation probability, $\rho_{gg}^{\text{therm}}(\infty)$ for a qubit in contact with a heat bath at temperature $T = eV/2$ (dashed).

B. Unravelling the master equation

Now that there are mutually distinguishable jumps, the conditional state of the qubit depends on the nature of the jump. We write

$$\tilde{\rho}_{1+c} = dt(\mathcal{J}[c_1]\rho_c(t) + \mathcal{J}[c_3]\rho_c(t)) \equiv dt\mathcal{J}^+\rho_c(t), \quad (38)$$

$$\tilde{\rho}_{1-c} = dt\mathcal{J}[c_2^\dagger]\rho_c(t) \equiv dt\mathcal{J}^-\rho_c(t), \quad (39)$$

where the subscript 1^+ indicates a lead electron tunnelling in the conventional (source to drain) direction, and 1^- indicates a lead electron tunnelling in the reverse direction, and we have defined \mathcal{J}^\pm for notational convenience later on.

To determine the evolution between jumps, we follow the same procedure as in section IV D to show that

$$\dot{\tilde{\rho}}_{0c}(t) = -i[H_{\text{sys}}, \tilde{\rho}_{0c}(t)] - (\mathcal{A}[c_1]\tilde{\rho}_{0c}(t) + \mathcal{A}[c_2^\dagger]\tilde{\rho}_{0c}(t) + \mathcal{A}[c_3]\tilde{\rho}_{0c}(t)). \quad (40)$$

VI. PSEUDO-THERMAL GROUND STATE OCCUPATION

We can use the unconditional master equation in each regime to compute the unconditional, steady-state probability of the qubit to be found in its ground state. It is given by $\rho_{gg}(\infty) = \langle g|\rho(\infty)|g\rangle$. From Eqs. (19) and (37), we see that $\rho_{gg}(\infty)$ is

$$\rho_{gg}(\infty) = \begin{cases} \frac{eV+\phi}{2eV} & \text{if } \phi < eV \\ 1 & \text{if } \phi > eV \end{cases} \quad (41)$$

In contrast, the ground state occupation of a qubit in thermal equilibrium with a heat bath at temperature T is given by $\rho_{gg}^{\text{therm}}(\infty) = \frac{e^{\phi/k_B T}}{1+e^{\phi/k_B T}}$. Figure 2 shows these two ground state probabilities for the case where $k_B T = eV/2$, and there is an evident analogy between the PC bias voltage and an external heat bath, however, we note that the leads are each nominally at zero temperature, that is $f_{S,D}(\omega) = \text{H}(\mu_{S,D} - \omega)$.

It has been suggested elsewhere that the PC bias acts somewhat like a heat bath¹¹, and we note that this correspondence is a natural conclusion of our analysis. It may be seen that even in the limit $eV \rightarrow 0$, the PC still causes the qubit to decay to its ground state, and we can see from Eq. (37) that in this limit, the energy relaxation time is given by $\tau_r^{-1} = 2\nu^2\phi \sin^2(\theta)$, and the dephasing time is $\tau_d^{-1} = 2\Gamma_d \cos^2(\theta) + \nu^2\phi \sin^2(\theta)$. When the PC bias voltage is zero, we see that $\tau_d = 2\tau_r$, indicating that the dephasing is solely due to energy relaxation. This zero-bias dephasing arising from relaxation is the solid state analogue of the optical decay of an atom in a vacuum.

This is a significant practical issue, since it means that the PC cannot be turned off merely by making the PC bias zero. To perform coherent quantum logic operations on the qubit in the presence of the PC will require an extra gate to control the PC tunnel rate. Then when the PC is off (i.e. $eV = 0$), $\nu^2\phi$ can be made much smaller than ϕ by a factor of order the fault tolerant threshold 10^{-4} , by raising the lead tunnel barrier.

VII. POWER SPECTRA OF CURRENT CORRELATIONS

Using the conditional master equations, we are able to evaluate the steady state power spectrum of the two time current correlation function

$$G(\tau) = E[I(t + \tau)I(t)] - E[I(t + \tau)]E[I(t)], \quad (42)$$

and we adopt the same procedure as described in the appendix of Goan and Milburn⁶. The power spectrum is the Fourier transform of this quantity,

$$S(\omega) = 2 \int_{-\infty}^{\infty} d\tau G(\tau) e^{-i\omega\tau} = \int_0^{\infty} d\tau G(\tau) \cos(\omega\tau), \quad (43)$$

since $G(\tau) = G(-\tau)$.

A. High bias power spectrum

To compute the steady state correlation function, we take the limit $t \rightarrow \infty$, so $\rho(t) \rightarrow \rho_{\infty}$. Using the relation $i dt = e dN(t)$, where $dN(t) \in \{0, 1\}$ is the number of electron tunnelling events in the time interval $(t, t + dt)$ and,

$$\begin{aligned} E[dN(t + \tau)dN(t)] &= \text{Prob}[dN(t) = 1]E[dN_c(t + \tau)|_{dN(t)=1}], \\ \text{Prob}[dN(t) = 1] &= \text{Tr} \{ \tilde{\rho}_{1c}(t + dt) \}, \\ E[dN_c(t + \tau)|_{dN(t)=1}] &= \text{Tr} \left\{ \sum_n \mathcal{J}[c_n] E[\tilde{\rho}_1 c(t + \tau)|_{dN(t)=1}] \right\}, \\ E[\tilde{\rho}_{1c}(t + \tau)|_{dN(t)=1}] &= e^{\mathcal{L}\tau} \tilde{\rho}_{1c}(t + dt) / \text{Tr} \{ \tilde{\rho}_{1c}(t + dt) \}, \\ dN(t)^2 &= dN(t), \end{aligned} \quad (44)$$

we obtain the correlation function in the high bias regime for $\tau > dt$

$$G_{\text{hb}}(\tau) = \begin{cases} e^2 (\text{Tr} \{ \sum_{n,n'} \mathcal{J}[c_n] e^{\mathcal{L}\tau} \mathcal{J}[c_{n'}] \rho_{\infty} \} - \text{Tr} \{ \sum_n \mathcal{J}[c_n] \rho_{\infty} \}^2) & \text{for } \tau > dt, \\ e^2 \text{Tr} \{ \sum_n \mathcal{J}[c_n] \rho_{\infty} \} \delta(\tau) & \text{for } \tau = dt. \end{cases} \quad (45)$$

We use Eq. (31) and the definitions of \bar{I}_{loc} and Δi to write $G_{\text{hb}}(\tau)$ in terms of \bar{I}_{loc} and δI_{loc} .

$$G_{\text{hb}}(\tau) = e(\bar{I}_{\text{loc}} - \delta I_{\text{loc}} \frac{\phi}{2eV} \cos(\theta)) \delta(\tau) + e^{-\Gamma_d \sin^2(\theta)\tau} e^2 \left(1 - \frac{\phi^2}{(eV)^2} \right) \nu^2 (2TeV \cos(\theta) + \nu\phi \sin^2(\theta))^2, \quad (46)$$

Dropping the small term $\nu\phi \sin^2(\theta)$, which is formally equivalent to keeping only the lowest order term in a series expansion in δI_{loc} , and taking the Fourier transform gives

$$S_{\text{hb}}(\omega) = S_0 - e\delta I_{\text{loc}} \frac{\phi}{V} \cos(\theta) + \frac{(\delta I_{\text{loc}})^2 \Gamma_d \left(1 - \frac{\phi^2}{(eV)^2} \right) \sin^2(2\theta)}{4(\Gamma_d^2 \sin^4(\theta) + \omega^2)} \quad (47)$$

where $S_0 = 2e\bar{I}_{\text{loc}}$.

B. Low bias power spectrum

The correlation function in the low bias regime turns out to be time independent. In this regime, there are two distinguishable jump processes that can occur: source to drain electron tunnelling (both elastic and inelastic), and drain to source tunnelling (inelastic only). Therefore the current is related to the number of jumps in the time interval by $i dt = e(dN^+(t) - dN^-(t))$, where $dN^{+(-)}(t)$ counts the number of source-to-drain (drain-to-source) tunnelling events in the time interval $(t, t + dt)$.

To evaluate the expectation values in $G(\tau)$, we use slightly generalised versions of Eqs. (44), for instance

$$\begin{aligned} \text{Prob}[dN^{\pm}(t) = 1] &= \text{Tr} \{ \tilde{\rho}_{1\pm c}(t + dt) \}, \\ E[dN_c^x(t + \tau)|_{dN^y(t)=1}] &= \text{Tr} \{ \mathcal{J}^x E[\tilde{\rho}_1 c(t + \tau)|_{dN^y(t)=1}] \} \text{ for } x, y = \pm. \end{aligned}$$

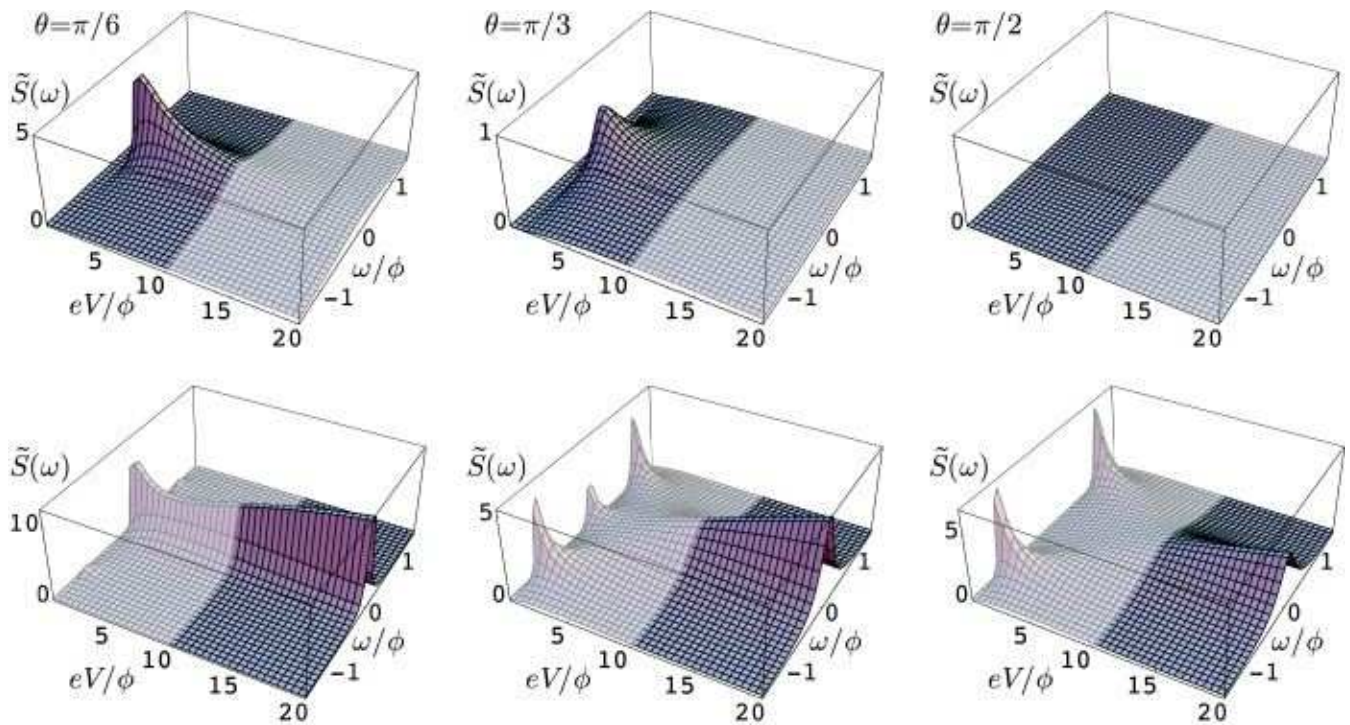


FIG. 3: Power spectra, $\tilde{S}(\omega)$, of current correlations calculated from Eqs. (47) and (50) (top row), and from⁶ (bottom row) as a function of eV/ϕ for $\theta = \pi/6, \pi/3$ and $\pi/2$. In all figures, $\nu^2 = 0.1$ for illustrative purposes. The greyed-out areas indicate regions for which the plotted power spectra are *not* valid: our calculations (top row) are valid for the sub-Zeno regime, $eV/\phi < 1/\nu^2 = 10$, whereas previous calculations (bottom row) are valid in the Zeno regime, $eV/\phi > 1/\nu^2 = 10$.

As before, to compute the steady state power spectrum, we make the replacement $\rho(t) \rightarrow \rho_\infty = |g\rangle\langle g|$, for the low bias regime. It is evident that $\mathcal{J}^- \rho_\infty = \mathcal{J}[c_2^\dagger] \rho_\infty = \mathcal{J}[c_1] \rho_\infty = 0$, so we find that

$$G_{\text{lb}}(\tau) = \begin{cases} e^2 (\text{Tr}\{\mathcal{J}[c_3] e^{\mathcal{L}\tau} \mathcal{J}[c_3] \rho_\infty\} - \text{Tr}\{\mathcal{J}[c_3] \rho_\infty\}^2) & \text{for } \tau > dt, \\ e^2 \text{Tr}\{\mathcal{J}[c_3] \rho_\infty\} \delta(\tau) & \text{for } \tau = dt. \end{cases} \quad (48)$$

$$= e^2 (\mathcal{T} + \nu \cos(\theta))^2 eV \delta(\tau) \quad (49)$$

Thus, the steady state low bias current correlation function is just due to elastic tunnelling through the PC. The low bias power spectrum is

$$S_{\text{lb}}(\omega) = S_0 - e \delta I_{\text{loc}} \cos(\theta) + O(\delta I_{\text{loc}}^2). \quad (50)$$

C. Comparison with previous results

The current correlation function, $G_{\text{GM}}(\tau)$, given in^{6,9} (subscript GM denotes the authors initials) is only valid for $\epsilon = 0$, but it is straightforward to calculate the general result, which is useful in order to compare our results with previous work. We present the general calculation in Appendix C. For the purposes of this section, we define a scaled power spectrum

$$\tilde{S}(\omega) = \frac{\phi}{\delta I_{\text{loc}}^2} (S(\omega) - S(\infty)). \quad (51)$$

Figure 3 shows a series of scaled power spectra, $\tilde{S}(\omega)$, calculated using Eqs. (47) and (50) in the top row, and from Goan and Milburn⁶ in the bottom row. Each figure shows how the power spectrum varies with increasing PC bias voltage, which enters the equations via the definition $\Gamma_d = 2eV\nu^2$.

The power spectrum calculated in this paper is very different from previous results. We have shown that there will never be an oscillatory response, in contrast to other work which predicted the presence of oscillations in the measured

current when $\Gamma_d \lesssim 2\phi$. In particular, there are discernible peaks in the power spectrum (away from $\omega = 0$) when $\Gamma_d < \sqrt{2}\phi$. The lack of oscillations is clear from the top row of Fig. 3 where the maximum power is concentrated around $\omega = 0$.

For illustrative purposes, we will take $\nu^2 = 0.1$ in what follows. The rotating wave approximation we used to derive our master equation is valid in the sub-Zeno regime, where $eV/\phi \ll 1/\nu^2 = 10$. In contrast previous results are only valid in the opposite regime $eV/\phi \gg 1/\nu^2 = 10$. For clarity, regions where the power spectra of Fig. 3 are not valid have been shaded lighter.

Figure 3 (bottom panels) shows that previous analyses predict the splitting of the DC peak into several AC peaks at low bias. The splitting occurs for $\nu^2 eV/\phi \leq 1/\sqrt{2}$, which is certainly well below the Zeno regime ($\nu^2 eV \gg \phi$). Arguably, it is on the threshold of the sub-Zeno regime ($\nu^2 eV \ll \phi$) that we are concerned with, where no splitting at low bias is evident (top panels).

In the transition between the sub-Zeno and Zeno regime, for which $\nu^2 eV \approx \phi$, we are unable to make any firm predictions, though it is reasonable to expect that the power spectrum will vary smoothly between the two limiting cases as eV/ϕ increases.

D. Steady state current

The steady state current is given by $I_{ss} = E[I(t)] = e \text{Tr}\{\sum_n \mathcal{J}[c_n] \rho_\infty\}$, which is proportional to the frequency independent part of the power spectrum, Eqs. (47) and (50). This agrees with other results in the literature^{22,23}. To first order in δI_{loc} , we find

$$I_{ss} = \begin{cases} \bar{I}_{loc} - \frac{\cos(\theta)\phi}{2eV} \delta I_{loc} = \bar{I}_{loc} - \frac{\epsilon}{2eV} \delta I_{loc} & \text{if } \phi < eV \\ \bar{I}_{loc} - \frac{\cos(\theta)}{2} \delta I_{loc} = \bar{I}_{loc} - \frac{\epsilon}{2\phi} \delta I_{loc} & \text{if } \phi > eV \end{cases} . \quad (52)$$

Using I_{ss} we can compute the DC conductance

$$G = i_{ss}/V = \begin{cases} \mathcal{T}^2 + \nu^2 + 2\nu\mathcal{T}\epsilon/(eV) & \text{if } \phi < eV, \\ \mathcal{T}^2 + \nu^2 + 2\nu\mathcal{T}\epsilon/\phi & \text{if } \phi > eV, \end{cases} .$$

in units of e^2/h . This indicates that the steady state current depends on the qubit bias ϵ . As ϵ varies the conductance changes accordingly, which is qualitatively in agreement with¹⁷.

VIII. MEASUREMENT TIME

The detector partially projects the qubit onto the energy eigenbasis, as seen in the form of jump operator c_3 . The energy eigenbasis is therefore the ‘preferred’ basis for the detector.

An important quantity of interest is the measurement time. This is the time taken for the measurement to project a qubit initially prepared in an equal superposition of energy eigenstates onto one or other of them. We therefore take $\rho(0) = (|e\rangle + |g\rangle)(\langle e| + \langle g|)/2$. Following Goan et al.⁷, we compute the rate of change of $E[dz_c^2(0)] \equiv E[\text{Tr}\{\sigma_z^{(e)} d\rho_c(0)\}^2]$.

We present the calculation for high bias, and note that we obtain the same result for low bias. Using the fact that

$$d\rho_c(t) = \rho_c(t+dt) - \rho_c(t) = dN(t)\rho_{1c}(t+dt) + (1-dN(t))\rho_{0c}(t+dt) - \rho_c(t), \quad (53)$$

$dN(t)^2 = dN(t)$ and $\text{Tr}\{\sigma_z^{(e)} \rho(0)\} = 0$, we find that to first order in dt

$$\begin{aligned} E[dz_c^2(0)] &= E[dN(0) \text{Tr}\{\sigma_z^{(e)} \rho_{1c}(dt)\}^2], \\ &= \frac{\text{Tr}\{\sigma_z^{(e)} \tilde{\rho}_{1c}(dt)\}^2}{\text{Tr}\{\tilde{\rho}_{1c}(dt)\}}, \\ &= 2\Gamma_d \cos(\theta)^2 dt + O(\nu^3 \phi). \end{aligned} \quad (54)$$

Thus the measurement time is $\tau_m^{-1} = 2\Gamma_d \cos(\theta)^2 + O(\nu^3 \phi)$. We note that $\tau_m \geq \tau_d$, with equality only when $\theta = 0$, indicating that the detector is inefficient unless the qubit energy eigenstates are localised.

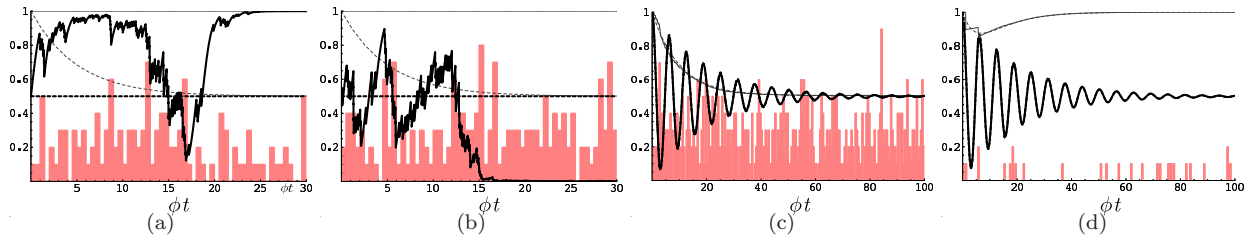


FIG. 4: (a) & (b) Showing distinct simulations where the qubit collapses to $|l\rangle$ and $|r\rangle$ respectively [for $\theta = 0$, $eV/\phi = 10$, $\nu^2 = 0.005$, $\mathcal{T}^2 = 0.5$]. At $\theta = \pi/2$ currents are uncorrelated with the qubit in either (c) high-bias [$eV/\phi = 10$, $\nu^2 = 0.005$, $\mathcal{T}^2 = 0.5$] or (d) low-bias [$eV/\phi = 0.5$, $\nu^2 = 0.05$, $\mathcal{T}^2 = 0.5$]. In all panels, dark curves are $\langle l|\rho_c(t)|l\rangle$ (solid) and $\langle l|\rho(t)|l\rangle$ (dashed), and light curves are the conditional purity $\text{Tr}\{\rho_c(t)^2\}$ (solid) and unconditional purity $\text{Tr}\{\rho(t)^2\}$ (dashed). Histograms show the number of jumps per time interval, (scaled by $1/10$).

IX. QUANTUM TRAJECTORIES

In Figs. 4(a) and 4(b) we show two different quantum trajectory simulations for $\theta = 0$, using the same parameters to generate both (see caption for values). We show the conditional probability (dark, solid line), $\langle l|\rho_c(t)|l\rangle$, and unconditional probability (dark, dashed line), $\langle l|\rho(t)|l\rangle$, of the qubit to be in the left well. Also shown is the purity of conditional state (light, solid), $\text{Tr}\{\rho_c(t)^2\}$, and of the unconditional state $\text{Tr}\{\rho(t)^2\}$, (light, dashed). We also show a histogram of the number of jump processes that were encountered in each time window, and this corresponds to experimentally measured currents. In all trajectories shown in this paper, the histograms are scaled by the factor $\frac{1}{10}$, and are mutually comparable. In these two figures, the initial state of the system is chosen to be the pure state $(|l\rangle + |r\rangle)/\sqrt{2}$.

The evolution of the measurement clearly shows the qubit collapsing to the state $|l\rangle$ or $|r\rangle$, and the state remains pure throughout. This is because, at $\theta = \pi/2$, the inelastic jump operators c_1 and c_2 are suppressed, and the remaining jump operator c_3 partially projects the state onto the localised basis. The average current, determined by the mean of the histogram is higher in the case where the qubit collapsed onto the state $|r\rangle$, which is consistent with physical intuition, since in this configuration, the tunnelling rate through the PC is highest. The fact that the unconditional probability to find the electron on the left well is constant at 0.5 reflects the fact that the state of the system collapses to $|l\rangle$ or $|r\rangle$ with equal probability, consistent with the initial state preparation being an equal superposition of the localised states, and thus for $\theta = 0$, the PC serves as a good quantum non-destructive (QND) measurement device.

Figures 4(d) and 4(c) shows the dynamics of the system for $\theta = \pi/2$ in the high bias ($eV/\phi = 2$) and low bias ($eV/\phi = 0.5$) regimes, respectively. In both cases, the initial state of the system is $|l\rangle$.

As predicted by Eq. (19), in the high bias limit the equilibrium state of the system is an unequal mixture of $|g\rangle$ and $|e\rangle$. We may calculate the unconditional steady state purity, and we find $\text{Tr}\{\rho(\infty)\} = \frac{(eV)^2 + \phi^2}{(2eV)^2} = 0.505$ for the parameters used. This agrees with the simulation of Fig. 4(d), where the conditional and unconditional evolution is very similar.

Similar comments apply to Fig. 4(c), however the unconditional steady state is always $|g\rangle$ for the low bias limit, which is of course a pure state, and for the case considered is just an equal superposition of localised states $|g\rangle = (|l\rangle + |r\rangle)/\sqrt{2}$. Thus the probability for the qubit to be in the left well is just the same as for Fig. 4(d), but the equilibrium state is pure.

We illustrate the effect of changing parameters in Fig. 5. We show simulated trajectories for five different bias voltages, $eV = 0.5, 1, 2$ and 4 , and for three different mixing angles $\theta = \pi/8, \pi/4$ and $3\pi/8$. In the high bias regime, and small values of θ there are fluctuations that bear a superficial resemblance to the quantum Zeno effect (QZE). The state of the qubit tends to fluctuate between mixtures of energy eigenstates, and the conditional density matrix is diagonal in the energy eigenbasis, with off-diagonal terms being negligible in this basis.

This resemblance to the QZE is only superficial however. In the QZE, the free dynamics of the qubit are suppressed due to the strong and frequent measurement which project the system into pure, localised states $\{|l\rangle, |r\rangle\}$. The sharp transitions that occur in the QZE result from the small probability for the electron to make a transition between sites which is realised as a rapid, occasional tunnelling event.

In contrast, the transitions that are evident in Fig. 5 for small θ are due to relaxation or excitation of the qubit, accompanied by inelastic tunnelling processes through the PC, rather than the ‘collapse of the wavefunction’ due to accumulated information about the qubit in the case of the QZE. As θ increases, the transitions become smaller in amplitude and less distinct, until $\theta = \pi/2$ when inelastic tunnelling events through the PC dominate the current and the qubit state is damped to the completely mixed state.

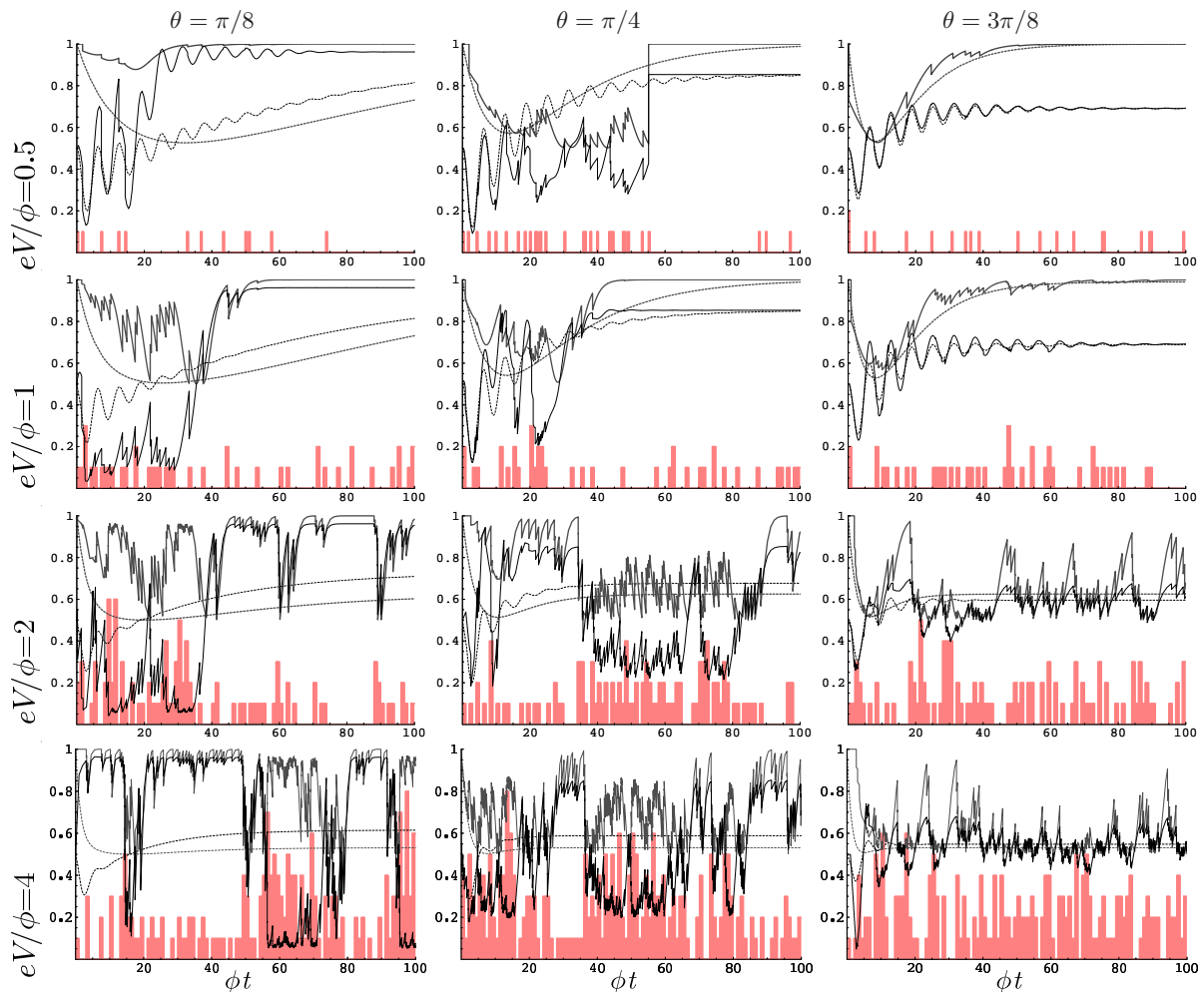


FIG. 5: Simulated trajectories from left to right, $\theta = \pi/8, \pi/4$ and $3\pi/8$. From top to bottom, $eV/\phi = 0.5, 0.9, 1.1, 2$ and 4 . In all $\nu^2 = 0.05$ and $\mathcal{T}^2 = 0.5$. In each panel, the dark curves are $\langle l|\rho_c(t)|l \rangle$ (solid) and $\langle l|\rho(t)|l \rangle$ (dashed), and the light curves are the purity of the conditional state $\text{Tr}\{\rho_c(t)^2\}$ (solid) and the unconditional state $\text{Tr}\{\rho(t)^2\}$ (dashed). The histogram shows the number of jumps that occurred in each time interval. The histograms are all scaled by the same factor, so are comparable with one another. Reverse tunnelling events are responsible for the sharp changes in the first two panels.

At the transition from low bias to high bias, $eV/\phi = 1$, fluctuations begin to appear in the steady state trajectory. For $eV < \phi$ the conditional steady state of the qubit is constant, whereas for $eV > \phi$ the conditional steady state shows fluctuations which increase with increasing bias voltage.

X. DISCUSSION

The predictions of this work should be experimentally verifiable. There are qualitative differences compared to previous work, notably the lack of coherent oscillations, as well as the sharp transition from the low- to high-bias regimes, at which point the power spectrum changes from being solely due to shot noise, to having some frequency dependence.

The master equation derived in this paper is not valid in the Zeno limit. We have shown that it is only in the Zeno limit that other analyses^{6,9,10,13} are valid. Thus, the results presented here describe accurately the dynamics of the measured qubit in the sub-Zeno regime. In the transition between the sub-Zeno and Zeno limits, where $\Gamma_d \approx \phi$, neither approach is formally valid, and non-Markovian effects may play a significant role. This transition is therefore an open area for investigation.

There are a number of practical issues that the present paper raises. Firstly, as discussed earlier, to turn the measurement off, it is not enough just to turn the PC bias to zero. Simultaneously one must also make ν^2 small,

which can be accomplished with extra surface gates.

Secondly, in order to perform a good QND measurement we require that $\tau_r \gg \tau_m^3$. From Eqs. (19), (37) and (54) we see that $\tau_r^{-1} = 2\nu^2 \max(\phi, eV) \sin^2(\theta)$ and $\tau_m^{-1} = 2\Gamma_d^2 \cos^2(\theta)$, so we require that $\sin(\theta) \approx 0$. Therefore, our work indicates that measurements in the sub-Zeno regime are not possible for highly delocalised qubit eigenstates. Furthermore, ideal measurements (i.e. measurements for which the conditional state remains pure) are only attainable when $\theta = 0$, so the energy eigenstates are the localised states.

In order to perform good QND type measurements, one could operate in the Zeno regime, though heating due to the large currents passing through the PC may be problematic^{17,24}. Alternatively performing a QND measurement in the sub-Zeno regime consists of three tasks:

1. Localise the qubit eigenstates by turning on the qubit bias (ϵ) and/or decreasing qubit tunnelling rate (Δ), so $\theta \approx 0$.
2. Increase the lead tunnelling rate (T_{00} and χ_{00}) by lowering a tunnel barrier.
3. Turn on the lead bias voltage (V).

The rate at which θ is varied effects a rotation on the qubit, so by selecting this rate appropriately, we can choose to measure in an arbitrary basis.

XI. CONCLUSION

In this paper we have used the quantum trajectories formalism to derived master equations for measurements of a charge qubit by an external point contact electrometer in the sub-Zeno regime. The master equation was derived without recourse to heuristic arguments, and resulted in the inclusion of incoherent jump processes, which whilst experimentally indistinguishable using current measurements, change the system dynamics dramatically. Furthermore, within the sub-Zeno regime, our results are valid for arbitrary detector bias voltage.

In the low-bias regime ($eV < \phi$) the qubit always relaxes to its ground state, much like a qubit in equilibrium with a zero-temperature bath. In this case, relaxation to the ground state is due to the eventual spontaneous relaxation of the qubit accompanied by an excitation of a PC lead electron. The corresponding steady state power spectrum is flat.

In the high-bias regime ($eV > \phi$) the PC leads act like a zero-entropy heat bath at non-zero temperature and both inelastic relaxation and excitation processes take place, causing the steady state of the qubit to be a mixture of excited and ground states. As the PC bias gets larger the relative fraction of each component of the mixture tends to 1/2, analogously to a qubit in contact with a heat bath at very high temperature.

Measurement remains possible in the sub-Zeno regime, with the added freedom that we may choose an arbitrary basis in which to measure.

A central claim in this paper is that the coherent qubit oscillations are suppressed by the inelastic processes. We have shown that previously predicted peaks^{6,9,10,13} in the steady state power spectrum of the PC current are not present when inelastic effects are correctly accounted for.

TMS thanks the Hackett Scholarships committee and the CVCP for financial support. SDB acknowledges support from the E.U. NANOMAGIQC project (Contract no. IST-2001-33186). We thank Bill Munro, Tim Spiller, Leonid Fedichkin, Hsi-Sheng Goan and Gerard Milburn for useful discussions.

APPENDIX A: EVALUATING THE t' INTEGRAL

Here we show explicitly how to evaluate the t' integral in Eq. (10). Firstly, from Eq. (9) or Eq. (11), we can see that $|\dot{\rho}_{i,j}(t)| \lesssim n\nu^2(eV + \phi)$, where $\nu = \sqrt{\pi g_S g_D / 2} \chi_{00}$ and $n = 3$ is the number of jump operators in $S(t)$. Then we can evaluate the time integral over t' in Eq. (9) by parts. For instance one such term is

$$\begin{aligned} \mathcal{I} &= \int_{-\infty}^t dt' e^{-i(\omega_k - \omega_q + \omega_m)t} e^{i(\omega_k - \omega_q + \omega_n)t'} P_m \rho(t') P_n^\dagger \\ &\approx e^{-i(\omega_k - \omega_q + \omega_m)t} P_m \left(\rho(t) \pi \delta(\omega_k - \omega_q + \omega_n) - \int_{-\infty}^t dt' \frac{e^{i(\omega_k - \omega_q + \omega_n)t'} \dot{\rho}(t')}{i(\omega_k - \omega_q + \omega_n)} \right) P_n^\dagger. \end{aligned}$$

\mathcal{I} appears within frequency integrals where $\omega_{k,q}$ are integrated over a range $\omega_k - \omega_q \leq eV$, so the size of the argument to the t' integral above is roughly $|\frac{\dot{\rho}(t')}{\omega_k - \omega_q + \omega_n}| \sim \frac{n\nu^2(eV + \phi)}{eV \pm \phi} \sim n\nu^2 \ll 1$, for operational parameter values. Thus the

integral term is small compared to the first term in braces, which is $O(1)$, so we have a very good estimate for the integral, given by

$$\mathcal{I} \approx \pi \delta(\omega_k - \omega_q + \omega_n) e^{i(\omega_n - \omega_m)t} P_m \rho(t) P_n^\dagger, \quad (\text{A1})$$

to within $O(\nu^2)$, and we have used this in Eq. (10).

Making the replacement $\rho(t') \rightarrow \rho(t)$, which is commonly done⁷, in Eq. (10) and evaluating the t' integral directly produces exactly the same result.

APPENDIX B: EVALUATING $\text{Tr}\{H_S \tilde{R}(t + dt)\}$

We now evaluate $\text{Tr}\{H_S \tilde{R}(t + dt)\}$ as an example to illustrate the derivation of Eqs. (23) and (24).

$$\begin{aligned} \text{Tr}\{H_S \tilde{R}(t + dt)\} &= \sum_{n, n'} \sum_{\omega, \omega', \omega''} \text{Tr}\{c_n \rho(t) c_{n'}^\dagger\} \text{Tr}\{a_D^\dagger(\omega' + \omega_n) \rho_D a_D(\omega'' + \omega_n)\} \\ &\quad \times \text{Tr}\{\omega a_S^\dagger(\omega) a_S(\omega) a_S(\omega') \rho_S a_S^\dagger(\omega'')\}, \end{aligned} \quad (\text{B1})$$

where $\rho_{S,D}$ are in Fermi distributions (at zero temperature, for our analysis), with different chemical potentials $\mu_{S,D}$, and is therefore diagonal in the energy basis. Note that

$$\begin{aligned} \text{Tr}\{\omega a_S^\dagger(\omega) a_S(\omega) a_S(\omega') \rho_S a_S^\dagger(\omega'')\} &= (1 - \delta_{\omega, \omega'}) \delta_{\omega', \omega''} \mathbf{H}_{\omega' \leq \mu_S} \mathbf{H}_{\omega \leq \mu_S}, \\ \text{Tr}\{a_D^\dagger(\omega' + \omega_n) \rho_D a_D(\omega'' + \omega_n)\} &= \delta_{\omega' + \omega_n, \omega'' + \omega_n} \mathbf{H}_{\omega' + \omega_n > \mu_D} \mathbf{H}_{\omega'' + \omega_n > \mu_D}, \end{aligned} \quad (\text{B2})$$

where $\delta_{\omega', \omega''}$ is the Kronecker-delta function, and $\mathbf{H}_{x < y}$ is the unit step function, which is unity when the inequality $x < y$ is satisfied and zero otherwise. Using these relations in Eq. (B1) gives

$$\begin{aligned} \text{Tr}\{H_S \tilde{R}(t + dt)\} &= \sum_n \sum_{\omega=0}^{\mu_S} \sum_{\omega'=\mu_D-\omega_n}^{\mu_S} \text{Tr}\{c_n \rho(t) c_{n'}^\dagger\} \omega (1 - \delta_{\omega, \omega'}) \\ &= \sum_n \text{Tr}\{\mathcal{J}[c_n] \rho(t)\} \sum_{\omega'=\mu_D-\omega_n}^{\mu_S} \left\{ \sum_{\omega=0}^{\mu_S} \omega - \omega' \right\} \end{aligned} \quad (\text{B3})$$

Similar arguments are used to compute $\text{Tr}\{H_D \tilde{R}(t + dt)\}$.

APPENDIX C: GENERALISED POWER SPECTRUM OF GOAN AND MILBURN⁶

The power spectra calculated in⁶ assumed $\epsilon = 0$. In order to compare our power spectra with theirs for arbitrary parameter values, we derive the power spectra for their model for arbitrary ϵ .

It is laborious to compute $G_{\text{GM}}(\tau)$ directly, however since we are only interested in the power spectrum, we can bypass the explicit solution for the correlation function in the time domain and calculate the power spectrum directly.

We wish to compute the Fourier transform, F , of equation (A8) of⁶ (hereafter called (GMA8)). This may be done via a Laplace transform, L , using the relation for a symmetric function $f(t)$

$$F_\omega[f(t)] = L_{i\omega}[f(t)] + L_{-i\omega}[f(t)]. \quad (\text{C1})$$

The Laplace transform of (GMA8) is

$$L_s[G_{\text{GM}}(\tau)] = e^{\bar{I}_{\text{loc}}} + \delta I_{\text{loc}}^2 (\text{Tr}\{n_1 L_s[e^{\mathcal{L}\tau} n_1 \rho_\infty]\} - \text{Tr}\{n_1 \rho_\infty\}^2 / s). \quad (\text{C2})$$

The notation $e^{\mathcal{L}\tau} n_1 \rho_\infty$ is just shorthand for the solution to the unconditional master equation (GM5a) at time τ subject to the initial condition $\rho(0) = n_1 \rho_\infty = n_1/2$. Taking the Laplace transform of (GM5a) gives

$$s L_s[\rho(t)] - \rho(0) = -i[H_{\text{sys}}, L_s[\rho(t)]] + \mathcal{D}[T_l + (T_r - T_l)n_1] L_s[\rho(t)]. \quad (\text{C3})$$

$L_s[\rho(t)]$ may be found straightforwardly from this expression and then $L_s[e^{\mathcal{L}\tau}n_1\rho_\infty]$ is obtained by substituting $\rho(0) \rightarrow n_1\rho_\infty = n_1/2$ into $L_s[\rho(\tau)]$, though it is a somewhat cumbersome expression. Evaluating the traces in Eq. (C2) yields

$$L_s[G_{GM}(\tau)] = \frac{e\bar{I}_{loc}}{2} + \delta I_{loc}^2 \frac{4s^2 + 2\phi^2 + 4s\mathcal{X}^2 + \mathcal{X}^4 + 2\phi^2 \cos(2\theta)}{4(4s^3 + 4s^2\mathcal{X}^2 + \phi^2\mathcal{X}^2 + s(4\phi^2 + \mathcal{X}^4) - \phi^2\mathcal{X}^2 \cos(2\theta))}, \quad (C4)$$

where we have used the same definition of \mathcal{X} as found in Goan and Milburn⁶, which for comparison is given in our notation as $\mathcal{X} = \nu\sqrt{eV}$. The power spectrum is then given by

$$S_{GM}(\omega) = 2F_\omega[G_{GM}(t)] = 2(L_{i\omega}[G_{GM}(\tau)] + L_{-i\omega}[G_{GM}(\tau)]) \quad (C5)$$

* Electronic address: tms29@cam.ac.uk

† Electronic address: sean.barrett@hp.com

¹ B. E. Kane, Nature **393**, 133 (1998).

² D. Loss and D. P. DiVincenzo, Phys. Rev. A **57**, 120 (1998).

³ Y. Makhlin, G. Schon, and A. Shnirman, Rev. Mod. Phys. **73**, 357 (2001).

⁴ W. Lu, Z. Ji, L. Pfeiffer, K. W. West, and A. J. Rimberg, Nature **423**, 422 (2003).

⁵ Y. A. Pashkin, T. Yamamoto, O. Astafiev, Y. Nakamura, D. V. Averin, and J. S. Tsai, Nature **421**, 823 (2003).

⁶ H.-S. Goan and G. J. Milburn, Phys. Rev. B **64**, 235307 (2001).

⁷ H.-S. Goan, G. J. Milburn, H. M. Wiseman, and H. B. Sun, Phys. Rev. B **63**, 125326 (2001).

⁸ S. A. Gurvitz, Phys. Rev. B **56**, 15215 (1997).

⁹ A. N. Korotkov, Phys. Rev. B **63**, 085312 (2001).

¹⁰ A. N. Korotkov and D. V. Averin, Phys. Rev. B **64**, 165310 (2001).

¹¹ D. Mozyrsky and I. Martin, Phys. Rev. Lett. **89**, 018301 (2002).

¹² S. Pilgram and M. Büttiker, Phys. Rev. Lett. **89**, 200401 (2002).

¹³ S. A. Gurvitz, L. Fedichkin, D. Mozyrsky, and G. P. Berman (2003), arxiv:cond-mat/0301409.

¹⁴ Y. Makhlin, G. Schon, and A. Shnirman, Phys. Rev. Lett. **85**, 4578 (2000).

¹⁵ M. Field, C. G. Smith, M. Pepper, D. A. Ritchie, J. E. F. Frost, G. A. C. Jones, and D. G. Hasko, Phys. Rev. Lett. **70**, 1311 (1993).

¹⁶ E. Buks, R. Schuster, M. Heiblum, D. Mahalu, and V. Umansky, Nature **391**, 871 (1998).

¹⁷ S. Gardelis, C. G. Smith, J. Cooper, D. A. Ritchie, E. H. Linfield, Y. Jin, and M. Pepper, Phys. Rev. B **67**, 073302 (2003).

¹⁸ J. M. Elzerman, R. Hanson, J. S. Greidanus, L. H. Willems van Beveren, S. DeFranceschi, L. M. K. Vandersypen, S. Tarucha, and L. P. Kouwenhoven, Phys. Rev. B **67**, 161308 (2003).

¹⁹ R. Aguado and L. P. Kouwenhoven, Phys. Rev. Lett. **84**, 1986 (2000).

²⁰ C. W. Gardiner and P. Zoller, *Quantum Noise* (Springer, 2000).

²¹ M. A. Nielsen and I. L. Chuang, *Quantum Computation and Quantum Information* (Cambridge University Press, 2000).

²² T. M. Stace and S. D. Barrett (2003), in review, see also cond-mat/0307727.

²³ H.-A. Engel, V. Golovach, D. Loss, L. M. K. Vandersypen, J. M. Elzerman, R. Hanson, and L. P. Kouwenhoven (2003), cond-mat/0309023.

²⁴ S. D. Barrett, Ph.D. thesis, University of Cambridge (2003).